Structural and functional consequences of the Milano mutation (R173C) in human apolipoprotein A-I

Eric T. Alexander,* Masafumi Tanaka,† Momoe Kono,† Hiroyuki Saito,† Daniel J. Rader,§ and Michael C. Phillips[1,*]

Gastroenterology/Nutrition/Hepatology Division,* Children's Hospital of Philadelphia, Department of Medicine,§ University of Pennsylvania School of Medicine, Philadelphia, PA 19104-4318; and Biophysical Chemistry Department,† Kobe Pharmaceutical University, Kobe 658-8558, Japan

Abstract **Carriers of the apolipoprotein A-I$_{Milano}$ (apoA-I$_M$) variant, R173C, have reduced levels of plasma HDL but no increase in cardiovascular disease. Despite intensive study, it is not clear whether the removal of the arginine or the introduction of the cysteine is responsible for this altered functionality. We investigated this question using two engineered variations of the apoA-I$_M$ mutation: R173S apoA-I, similar to apoA-I$_M$ but incapable of forming a disulfide bond, and R173K apoA-I, a conservative mutation. Characterization of the lipid-free proteins showed that the order of stability was wild type≈R173K>R173S>R173C. Compared with wild-type apoA-I, apoA-I$_M$ had a lower affinity for lipids, while R173S apoA-I displayed intermediate affinity. The in vivo effects of the apoA-I variants were measured by injecting apoA-I-expressing adeno-associated virus into apoA-I-null mice. Mice that expressed the R173S variant again showed an intermediate phenotype. Thus, both the loss of the arginine and its replacement by a cysteine contribute to the altered properties of apoA-I$_M$. The arginine is potentially involved in an intrahelical salt bridge with E169 that is disrupted by the loss of the positively charged arginine and repelled by the cysteine, destabilizing the helix bundle domain in the apoA-I molecule and modifying its lipid binding characteristics.—**Alexander, E. T., M. Tanaka, M. Kono, H. Saito, D. J. Rader, and M. C. Phillips. **Structural and functional consequences of the Milano mutation (R173C) in human apolipoprotein A-I. *J. Lipid Res.* 2009.** 50: **1409–1419.**

Supplementary key words high density lipoprotein • cholesterol • lipoprotein • protein structure

Apolipoprotein A-I (apoA-I), an amphipathic protein secreted by the liver and small intestine, is the major protein component of HDL (1). Plasma apoA-I and HDL cholesterol levels are inversely associated with the risk of cardiovascular disease (2). The anti-atherogenic properties of apoA-I are thought to arise from its central role in reverse cholesterol transport, the pathway by which excess cholesterol is effluxed from peripheral tissues and transported to the liver, where it is subsequently excreted from the body (2–4). The influence of apoA-I structure on its performance in reverse cholesterol transport is not well understood.

A powerful way to examine the structure-function relationship of a protein is to study the effects of genetic variants, especially ones that occur naturally and cause a phenotype in humans. In the case of apoA-I, the first known natural mutant is apoA-I$_M$ that is characterized by the mutation R173C (5). The introduction of a cysteine residue allows apoA-I to form apoA-I$_{Milano}$ (apoA-I$_M$) homodimers or heterodimers with apoA-II (6). The apoA-I$_M$ mutation is located in the N-terminal helix bundle domain of the protein (7, 8). Naturally occurring variants of apoA-I between residues 121 and 186 are often associated with low apoA-I levels (9). Individuals heterozygous for the apoA-I$_M$ mutation have very low plasma apoA-I and HDL cholesterol levels as well as moderately elevated triglycerides (10). Low levels of apoA-I$_M$ in plasma are likely due to reduced LCAT activation (11), which can lead to higher catabolic turnover of apoA-I (12, 13). Despite a lipid profile that is usually associated with a high risk of premature cardiovascular disease, apoA-I$_M$ carriers display no increase in cardiovascular disease or events (10, 14, 15). This has led to speculation that apoA-I$_M$ is a gain-of-function mutation that has enhanced cardio-protective effects (16–22), while others believe that wild-type (WT) apoA-I and apoA-I$_M$ are functionally equivalent (23, 24). A clinical trial of repeated intravenous infusions of

This work was supported by American Heart Association Grant 0625372U, National Institutes of Health Grant HL-22633, the Takeda Science Foundation, and the Suzuken Memorial Foundation.

Manuscript received 7 November 2008 and in revised form 15 December 2008 and in re-revised form 13 March 2009.

Published, JLR Papers in Press, March 24, 2009.
DOI 10.1194/jlr.M800578-JLR200

Abbreviations: AAV, adeno-associated virus; apo, apolipoprotein; ANS, 8-anilino-1-naphthalensulfonic acid; CD, circular dichroism; DMPC, dimyristoylphosphatidylcholine; GdnHCl, guanidine hydrochloride; ITC, isothermal titration calorimetry; PC, phosphatidylcholine; SUV, small unilamellar vesicles; Trx, thioredoxin; WT, wild type.

[1] To whom correspondence should be addressed.
e-mail: phillipsmi@email.chop.edu

apoA-I_M-phospholipid complexes demonstrated regression of existing atheromas after five weekly treatments (25, 26).

To date, it has not been determined how the R173C substitution is responsible for altering the functional aspects of the apoA-I_M mutant. For instance, is it the removal of the arginine and the loss of positive charge at position 173 or the introduction of a cysteine residue with the ability to form disulfide bonds that is responsible? To investigate this question, we generated two engineered variants of the apoA-I_M mutation, R173S apoA-I, a mutation structurally similar to apoA-I_M but without the ability to form disulfide bonds, and R173K apoA-I, a conservative mutation that maintains the positive charge at position 173 of WT apoA-I. The physical properties of these engineered mutants and their effects on plasma lipid levels and HDL composition in vivo via virus-mediated gene transfer were compared with WT and R173C apoA-I. Adeno-associated virus (AAV) vectors that have been shown to be capable of long-term hepatic expression of WT apoA-I (27) in mice were used in these experiments.

MATERIALS AND METHODS

Preparation of apoA-I mutants

To express human WT apoA-I and engineered variants, the cDNA of interest was cloned into the multiple cloning sites of the pET32a (+) vector, and the target protein was expressed as a histidine-tagged fusion protein with the 109-amino-acid thioredoxin (Trx) at the N terminus (7, 28). The resulting plasmids were transformed into *Escherichia coli* strain BL21(DE3). These transformed cells were cultured in Luria-Bertani medium at 37°C, and expression of the fusion protein Trx-apoA-I was induced with isopropyl-β-D-thiogalactopyranoside for 3 h. After sonicating the bacterial pellet, the lysate was centrifuged and the supernatant loaded onto a nickel-chelating, histidine binding resin column (Novagen). The Trx-apoA-I fusion protein bound to the column was eluted, pooled, and dialyzed against 20 mM NH_4HCO_3. Subsequently, the fusion protein was complexed with dimyristoylphosphatidylcholine (DMPC) to prevent nonspecific cleavage and then cleaved with thrombin to release the Trx. The mixture was then lyophilized, delipidated, and dissolved in 6 M guanidine hydrochloride (GdnHCl) solution. Trx was separated from apoA-I by gel filtration chromatography on a Sephacryl S-300 column. Further purification (>95%) of the proteins was done by gel filtration with Superdex 75 and/or anion exchange chromatography with Q-Sepharose. Purity was confirmed by SDS-PAGE (data not shown). ApoA-I_M was present in both monomeric and disulfide-linked forms; fractions corresponding to dimeric apoA-I_M were pooled separately and confirmed to be >95% dimeric apoA-I_M by SDS-PAGE (data not shown). All proteins were stored at −80°C in lyophilized form and before use were dissolved in the appropriate buffer containing 6 M GdnHCl and dialyzed extensively before use.

Circular dichroism spectroscopy

The α-helix contents of the apoA-I variants were determined by obtaining far-UV circular dichroism (CD) spectra from 184–260 at room temperature using a Jasco J-600 spectropolarimeter. The proteins were dissolved in 6 M GdnHCl (for monomeric apoA-I_M, 1% β-mercaptoethanol was added to the GdnHCl solution to reduce C173 completely), dialyzed overnight against excess 10 mM sodium phosphate buffer (pH 7.4), and diluted to 25–50 μg/ml for obtaining the CD spectrum. For apoA-I/small unilamellar vesicle (SUV) mixtures, apoA-I was incubated for 1 h prior to the measurement with egg phosphatidylcholine (PC) SUV prepared by sonication as described before (29). The CD spectra were corrected by subtracting the baseline for an appropriate blank sample. The α-helix content was calculated from the molar ellipticity at 222 nm ($[\theta]_{222}$) using the equation: percentage α-helix = $[(-[\theta]_{222} + 3000)/36000 + 3000] \times 100$ (30, 31). Thermal denaturation was monitored from the change in $[\theta]_{222}$ as the sample was heated at 1°/min over the temperature range 20–90°C, as described (32).

Isothermal denaturation studies

The effect of GdnHCl or urea concentration on the reversible unfolding of apoA-I secondary structure was monitored by CD spectroscopy using $[\theta]_{222}$ (31, 33) and by measuring the change in tryptophan fluorescence emission intensity at 335 nm with a Hitachi F-4500 fluorescence spectrophotometer using an excitation wavelength of 295 nm to avoid tyrosine fluorescence (33, 34). Proteins at a concentration of 50 μg/ml in Tris buffer (10 mM Tris-HCl, 150 mM NaCl, 0.02% NaN_3, and 1 mM EDTA, pH 7.4) were incubated overnight at 4°C with GdnHCl or urea at various concentrations. The equilibrium constants (K_d) describing the unfolding of apoA-I at given denaturant concentrations were calculated as described before (35) using either $[\theta]_{222}$ or the change in tryptophan fluorescence emission intensity at 335 nm (7, 33). The free energy of denaturation, $\Delta G°_D$ and the midpoint of denaturation were determined by the linear equation, $\Delta G_D = \Delta G°_D - m[\text{denaturant}]$, where $\Delta G_D = -RT \ln K_d$ and m reflects the cooperativity of denaturation in the transition region (7, 35).

8-Anilino-1-naphthalensulfonic acid fluorescence measurements

The 8-anilino-1-naphthalensulfonic acid (ANS) fluorescence measurements were carried out with a Hitachi F-4500 fluorescence spectrophotometer. In all experiments, the apoA-I was freshly dialyzed from a 6 M GdnHCl solution into a Tris buffer (10 mM Tris-HCl, 150 mM NaCl, 0.02% NaN_3, and 1 mM EDTA, pH 7.4) before use. The extent of ANS binding to hydrophobic sites on the apoA-I variants at 25°C was determined by measuring ANS fluorescence spectra recorded from 400 to 600 nm at an excitation wavelength of 395 nm, in the absence or presence of 50 μg/ml protein and an excess of ANS (250 μM) (7, 31).

DMPC clearance assay

The kinetics of solubilization of DMPC multilamellar vesicles by the apoA-I variants were measured by monitoring the decrease in absorbance at 325 nm, as described previously (36). The time courses of decrease in absorbance with time were fitted to a monoexponential decay equation, and the clearance rates were compared in terms of the product (rate constant X fraction of absorbance cleared at equilibrium) normalized to WT apoA-I (7).

Isothermal titration calorimetry measurements

Heats of apoA-I binding to egg PC SUV at 25°C were measured with a MicroCal MCS isothermal titration calorimeter (29). To ensure that the injected protein bound completely to the SUV surface, the PC-to-protein molar ratio was kept over 10,000. The decay rate constants for the heats of binding were obtained from fitting the titration curves to a one-phase exponential decay model.

Preparation of apoA-I AAV

WT apoA-I cDNA was mutated using the Quikchange site-directed mutagenesis kit from Stratagene. Specific primers were designed

to mutate the WT apoA-I cDNA in the pAAVmcs plasmid (37). The plasmid containing the WT apoA-I cDNA served as the template for the mutagenic PCR reaction. After the PCR reaction, the sample was digested with Dpn I, an endonuclease specific for methylated and hemimethylated DNA, to digest the parental DNA template and select for mutation-containing synthesized DNA. The purified mutant plasmid was then transformed into XL1-Blue supercompetent cells. Several colonies were isolated and used to inoculate Luria-Bertani media containing 100 mg/ml ampicillin. The resulting plasmids were sequenced and restriction digested to confirm the presence of the intended mutation. The plasmid containing the mutant sequence was then submitted to the University of Pennsylvania Vector Core for use in creating the apoA-I AAV. All AAV were manufactured using triple-plasmid transfection of adherent human 293 cells using Ad helper, *trans*-packaging, and AAV vector plasmids. The AAV were purified from harvested lysates using ion exchange column chromatography as described previously (38). The human apoA-I AAV, and variants, contain the human apoA-I cDNA insert followed by a SV-40 poly(A) tail and are driven by the liver-specific human thyroglobulin promoter. The AAV were produced with a chimeric packaging construct in which the AAV2 rep gene was fused with the cap gene of AAV serotype 8 (37, 39).

Preparation and bleeding of WT apoA-I and apoA-I variant transgenic mice

ApoA-I $^{-/-}$ mice (8–12 weeks old, C57/Bl6 background; Jackson Laboratories) fed a chow diet were injected intraperitoneally with 1×10^{12} particles of apoA-I_M AAV, R173S, R173K, WT apoA-I AAV, or LacZ AAV with a total of five mice per group. Blood was drawn from the retro-orbital plexus after 4 h of daytime fasting and allowed to clot for 1 h at 4°C. The blood was then spun (10,000 rpm, 7 min, 4°C) to isolate the serum. Total cholesterol, HDL cholesterol, phospholipid, and human apoA-I levels were measured on a Cobas Fara (Roche Diagnostics Systems) using Sigma Diagnostics reagents. HDL for compositional analysis was obtained by adding 40 μl of polyethylene glycol to 100 μl of serum and incubating at 4° for 30 min (40). Samples were spun down (10,000 rpm, 7 min, 4°C) and the serum collected and analyzed using the Cobas Fara. A pool of 120 μl of plasma from six mice was diluted 2-fold with fast-protein liquid chromatography column buffer (1 mM EDTA and 154 mM NaCl, pH 8.0). Two hundred microliters of diluted sample were run on a Superose 6 column at a flow rate of 0.4 ml/min, and 0.5 ml fractions were collected. All animal protocols were approved by the University of Pennsylvania Institutional Animal Care and Use Committee.

Electrophoresis and Western blotting

Plasma samples (1 μl) were resolved on 4–20% nondenaturing, Tris-glycine gradient gels (Invitrogen) or 4–12% SDS-PAGE Tris-glycine gels (Invitrogen) and transferred to a nitrocellulose membrane. A polyclonal goat anti-human apoA-I antibody (K45252G; Biodesign) was used as the primary antibody at a dilution of 1:5,000, while a peroxidase-conjugated donkey anti-goat IgG (705-035-147; Jackson Immuno Research) was used as the secondary antibody at a dilution of 1:25,000. Blots were developed using chemiluminescence. The HDL fraction (density = 1.073–1.21 g/ml) was isolated by ultracentrifugation (41) of pooled plasma samples from mice expressing either WT human apoA-I or one of the variants. The isolated HDL were then run on 8–25% SDS-PAGE Phastgels (GE Healthcare) and stained for protein with Coomassie blue.

TABLE 1. Physical properties of apoA-I variants

ApoA-I Variants	Lipid-Free α-Helicity (%)[a]	Lipid-Bound α-Helicity (%)[b]	ANS Fluorescence Intensity[c]
WT	44 ± 4	70 ± 4	1.0
R173K	44 ± 3	74 ± 1	1.1
R173S	44 ± 1	72 ± 3	1.2
Milano (monomer)	42 ± 4	65 ± 8	1.6
Milano (dimer)	33 ± 2[d]	45 ± 6[d]	1.6

[a] Mean ± SD from at least four independent measurements.
[b] Mean ± SD from three independent measurements. ApoA-I bound to egg PC SUV at a 60:1 (PC:apoA-I) molar ratio.
[c] Values are ratios to WT apoA-I. Error is within 0.1.
[d] $P < 0.01$ compared with WT apoA-I.

RESULTS

Secondary structure of apoA-I variants

The secondary structures of apoA-I variants were analyzed by far-UV CD spectroscopy. The α-helix contents of lipid-free, monomeric apoA-I_M and both R173K apoA-I and R173S apoA-I were no different than WT (**Table 1**); this finding is consistent with earlier comparisons of apoA-I_M and WT apoA-I (42, 43). Interestingly, the dimeric form of lipid-free apoA-I_M was significantly less α-helical than WT apoA-I, indicating that the presence of a disulfide bond at position 173 disrupts the WT secondary structure. The α-helicity in the lipid-bound state follows a similar pattern, with only the lipid-bound dimeric apoA-I_M showing a reduction in α-helicity compared with WT apoA-I (Table 1). An earlier study by Calabresi et al. (44) showed that dimeric apoA-I_M in both the lipid-free and lipid-bound states was more α-helical than WT apoA-I. This difference to our results is perhaps due to enhanced self-association at the higher concentration of dimeric apoA-I_M that the authors used to measure α-helicity.

Thermal unfolding and GdnHCl and urea denaturation of apoA-I variants

Figure 1 shows the thermal denaturation curves of WT apoA-I, R173S apoA-I, and monomeric apoA-I_M monitored

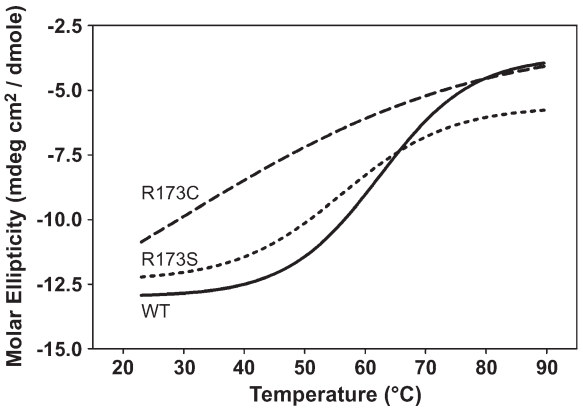

Fig. 1. Thermal unfolding of apoA-I variants monitored by changes in the molar ellipticity at 222 nm. Thermal denaturation was monitored by the change in molar ellipticity at 222 nm over the temperature range of 20–90°C of apoA-I solutions (50 μg/ml) in sodium phosphate buffer (pH 7.4). WT apoA-I (solid line), monomeric apoA-I_{Milano} (dashed line), and R173S apoA-I (dotted line).

TABLE 2. Stability of apoA-I variants

ApoA-I Variants	Midpoint of Thermal Denaturation (°C)[a]	Midpoint of GdnHCl Denaturation (M)[a]	$\Delta G°_D$ (kcal/mol)[b]	Midpoint of GdnHCl Denaturation (M)[a]	$\Delta G°_D$ (kcal/mol)[b]	Midpoint of Urea Denaturation (M)[a]	$\Delta G°_D$ (kcal/mol)[b]
	Molar Ellipticity at 222 nm			Fluorescence Intensity[c]			
WT	60	1.0	3.9 ± 0.2	1.0	4.6 ± 0.3	3.0	6.2 ± 0.2
R173K	61	1.0	3.9 ± 0.2	1.1	4.5 ± 0.2	2.7[d]	5.8 ± 0.2
R173S	56[d]	0.9	3.3 ± 0.1[d]	1.0	3.7 ± 0.1[d]	2.2[d]	4.1 ± 0.1[d]
Milano (monomer)	53[d,e]	0.8[d]	2.4 ± 0.2[d,e]	0.9	2.3 ± 0.1[d,e]	1.6[d,e]	1.8 ± 0.1[d,e]
Milano (dimer)	56[d,e]	0.8[d]	0.9 ± 0.1[d,e]	0.9[d]	1.9 ± 0.1[d,e]	2.0[d,e]	2.2 ± 0.1[d,e]

[a] Average of at least four measurements which differed by <0.4%. ApoA-I variants in lipid-free state.
[b] Free energy of denaturation listed as a mean ± SD, n = 3–5.
[c] Change in Trp fluorescence intensity at 335 nm.
[d] $P < 0.01$ compared with WT apoA-I.
[e] $P < 0.01$ compared with each other.

by the change in molar ellipticity at 222 nm over the temperature range 20–90°C. In comparison to the denaturation curve of WT apoA-I, both R173S apoA-I and monomeric apoA-I_M displayed a decrease in the cooperative nature of unfolding as indicated by the shallowness of their denaturation curves (Fig. 1). The midpoints of thermal denaturation are summarized in **Table 2**. The introduction of the apoA-I_M mutation destabilized the protein in both the monomeric and dimeric forms; a lower free energy of unfolding of monomeric apoA-I_M compared with WT apoA-I has been reported previously (43). The R173S mutation also destabilized apoA-I. The conservative mutation, R173K, had no effect on the stability of apoA-I as measured by thermal denaturation (data not shown).

GdnHCl-induced denaturation profiles were monitored by the molar ellipticity at 222 nm as well as by decreases in tryptophan fluorescence emission intensity. These changes in tryptophan fluorescence measure the stability of the N-terminal helix bundle because apoA-I contains four tryptophan residues, all of which are located in the helix bundle domain, whereas molar ellipticity measures the unfolding of all α-helices in the protein molecule. In **Fig. 2**, the denaturation curves of both monomeric and dimeric apoA-I_M as well as R173S apoA-I are shifted to lower concentrations of GdnHCl compared with WT apoA-I, indicating decreased structural stability. The dimeric apoA-I_M displayed a decrease in the cooperative nature of unfolding as indicated by the shallowness of its denaturation curve (Fig. 2). The conformational stability, $\Delta G°_D$, and the midpoint of GdnHCl denaturation were determined from linear plots of the Gibbs free energy against the GdnHCl concentration and are listed in Table 2. The monomeric and dimeric apoA-I_M mutant exhibited a significantly decreased $\Delta G°_D$ and midpoint of GdnHCl denaturation compared with WT apoA-I, indicating a reduction in stability. Similar to the results for thermal unfolding, R173S apoA-I also demonstrated a decrease in $\Delta G°_D$ and midpoint of GdnHCl denaturation, whereas R173K apoA-I was no different to WT apoA-I.

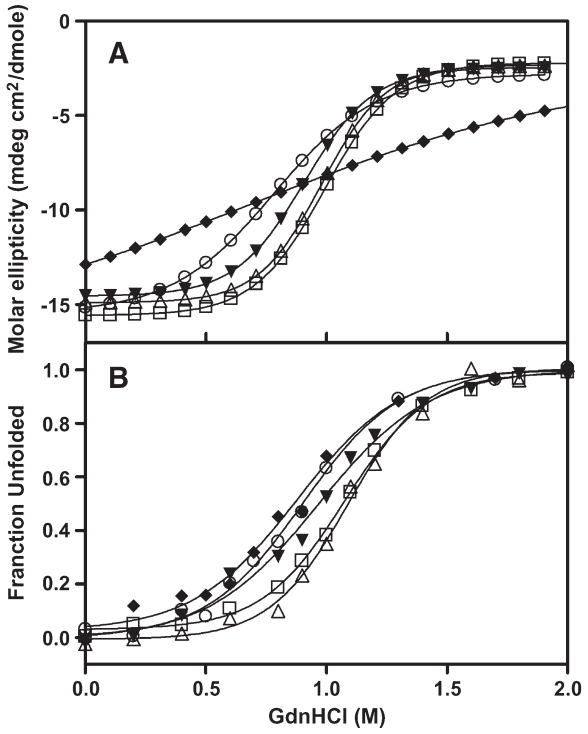

Fig. 2. GdnHCl denaturation of the apoA-I variants monitored by changes in the molar ellipticity at 222 nm and Trp fluorescence intensity. GdnHCl denaturation measured by change in molar ellipticity at 222 nm (A) and the change in tryptophan fluorescence emission intensity at 335 nm (B). WT apoA-I (open squares), apoA-I_{Milano} monomer (open circles), apoA-I_{Milano} dimer (diamonds), R173S apoA-I (closed triangles), and R173K apoA-I (open triangles).

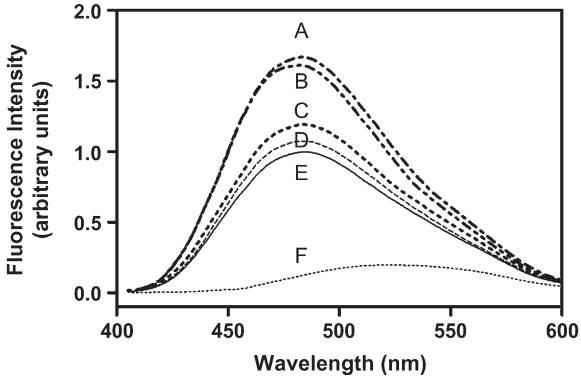

Fig. 3. ANS fluorescence spectra in the presence of apoA-I variants. The extent of ANS binding to hydrophobic sites on the apoA-I variants was determined by measuring ANS fluorescence spectra recorded from 400 to 600 nm at an excitation wavelength of 395 nm, in the absence or presence of 50 μg/ml protein and an excess of ANS. A: apoA-I_{Milano} monomer; B: apoA-I_{Milano} dimer; C: R173S apoA-I; D: R173K apoA-I; E: WT apoA-I; F: free ANS for comparison.

TABLE 3. DMPC clearance rate and ITC parameters of SUV binding of apoA-I variants

ApoA-I Variants	DMPC Clearance Rate[a]	ΔH (kcal/mol)[b]	Decay rate[b,c]
WT	1.0	−92.6 ± 5.3	1.0
R173K	1.2	−94.7 ± 5.7	1.0
R173S	1.1	−88.1 ± 5.8[d]	1.5
Milano (monomer)	1.0	−70.6 ± 5.5[d]	2.2
Milano (dimer)	0.5	−64.2 ± 3.7[d]	2.7

[a] Relative rate of DMPC clearance compared with WT apoA-I. Average of 8 to 12 runs per sample.
[b] Parameters of egg PC SUV binding from ITC, mean ± SD (n = 4–6).
[c] Values are ratios to WT apoA-I; estimated error is within ± 0.05. The rate constant for WT apoA-I was 1.19 ± 0.03 min^{-1}.
[d] $P < 0.01$ compared with WT apoA-I.

Urea-induced denaturation profiles were monitored by changes in tryptophan fluorescence emission intensity. GdnHCl denaturation measures only the contribution of hydrophobic or nonionic interactions to the stability of a protein due to the fact that electrostatic interactions between amino acids are masked by the ionic denaturant, whereas urea denaturation measures the contributions of both hydrophobic and electrostatic interactions (45). The conformational stability, $\Delta G°_D$, and the midpoint of urea denaturation were determined as described in Materials and Methods and are listed in Table 2. Similar to the results for thermal unfolding and GdnHCl denaturation, urea-induced denaturation indicates that R173S apoA-I was less stable than WT apoA-I and R173K apoA-I but more stable than monomeric and dimeric apoA-I_M. Of particular interest was the observation that when electrostatic interactions were taken into account (urea denaturation), the monomeric form of apoA-I_M was significantly less stable than dimeric form of apoA-I_M (Table 2).

ANS binding

ANS binding studies were performed to compare the exposure of hydrophobic regions in the apoA-I variants to the aqueous environment. When compared with ANS fluorescence in the absence of a protein, WT apoA-I induced a 5-fold increase in fluorescence intensity (**Fig. 3**), indicating the presence of ANS accessible hydrophobic surface (7, 31, 46, 47). The apoA-I_M mutation led to large increases in ANS fluorescence compared with WT apoA-I (Table 1), indicating that the inclusion of a cysteine at position 173 disturbs the tertiary structure of the protein, exposing more hydrophobic surface. The R173S mutation also increased the ANS fluorescence compared with WT apoA-I, but not to the same extent as apoA-I_M. The ANS fluorescence with R173K apoA-I was similar to that of WT apoA-I.

Interactions of apoA-I variants with lipid

We used a DMPC clearance assay to assess the abilities of the apoA-I variants to bind to, and solubilize, DMPC vesicles. As shown in **Table 3**, only the dimeric form of apoA-I_M exhibited slower kinetics of solubilization than WT apoA-I, indicating that the presence of a disulfide bond linking two apoA-I_M molecules at position 173 impairs the protein's ability to solubilize the DMPC vesicles. All other variants of apoA-I had the same ability as WT apoA-I to solubilize DMPC vesicles. Earlier studies have given conflicting results regarding the relative abilities of apoA-I_M and WT apoA-I to solubilize DMPC vesicles. One group determined that monomeric apoA-I_M cleared DMPC vesicles as efficiently as WT apoA-I (43), in agreement with our results. However, a second group determined that monomeric apoA-I_M was more efficient at clearing DMPC vesicles than WT apoA-I and that dimeric apoA-I_M was as efficient as WT apoA-I (42, 48). These discrepancies may be due to the fact that a single concentration of apoA-I was used, whereas our values were derived using a range of apoA-I concentrations.

To further characterize the interactions of apoA-I variants with lipid, we measured the heats of binding of apoA-I to egg PC SUV using isothermal titration calorimetry (ITC) (7, 49). Because there is no morphological change in the SUV particles when apoA-I binds, the heat change upon apoA-I binding contains contributions from protein-lipid interaction and conformational rearrangement of apoA-I (50). The binding enthalpies at low surface concentrations of the proteins are given in Table 3. The apoA-I_M mutation resulted in a decreased binding enthalpy compared with WT apoA-I; the dimeric form of the protein showed a similar reduction to the monomeric form. The R173S apoA-I variant displayed a small but significant decrease in enthalpy compared with WT apoA-I, whereas the R173K mutation had no effect on the binding enthalpy. The exothermic enthalpy of binding is the major component of the favorable free energy of binding of apoA-I to SUV, and the increase in α-helix content associated with such binding is largely responsible for this enthalpy (29, 51). Thus, the reductions in enthalpy compared with WT apoA-I shown in Table 3 are a consequence of a smaller increase in α-helix content upon lipid interaction. The results of CD

TABLE 4. Plasma apoA-I and lipid levels

AAV[a]	ApoA-I (mg/dl)	HDL Cholesterol (mg/dl)	Total Cholesterol (mg/dl)	Cholesteryl Ester (%)	Phospholipids (mg/dl)	Triglycerides (mg/dl)
WT apoA-I	154 ± 4	80 ± 13	104 ± 13	73 ± 2	199 ± 23	41 ± 5
apoA-I_{Milano}	121 ± 9[b]	31 ± 2[b]	44 ± 14[b]	65 ± 2[b]	139 ± 11[b]	61 ± 22
R173S apoA-I	115 ± 10[b]	48 ± 5[b]	63 ± 8[b]	71 ± 3	133 ± 17[b]	40 ± 14
R173K apoA-I	147 ± 16	81 ± 13	105 ± 18	72 ± 2	190 ± 30	35 ± 9
LacZ	0 ± 0[b]	14 ± 1[b]	20 ± 3[b]	66 ± 4[b]	69 ± 11[b]	31 ± 4

[a] Respective AAV injected into apoA-$I^{-/-}$ mice with a dose of 1.0×10^{12} viral particles. All data taken from week 6 postinfection (except percentage cholesteryl ester, week 10) and represent a mean ± SD (n = 5).
[b] $P < 0.001$ compared with WT.

measurements confirmed that the increase in α-helix content upon SUV binding was less for apoA-I_M than for WT apoA-I (Table 1).

Significant differences in the decay rates of the isothermal titration curves were observed between the apoA-I variants. As shown in Table 3, the decay rate was increased in the R173S apoA-I mutant and further increased for the monomeric and dimeric apoA-I_M mutant. We also observed strong inverse correlations between the midpoint of thermal denaturation and the ITC decay rate as well as the midpoint of GdnHCl denaturation (Table 2) and the ITC decay rate (data not shown). These results suggest that the stability of the apoA-I molecule modulates its rate of conformational rearrangement on the surface of SUV particles.

In vivo apoA-I and plasma lipid levels

ApoA-I-null mice were injected intraperitoneally with 1×10^{12} viral particles of the appropriate AAV. Six weeks postinjection, plasma from mice expressing the LacZ control had no detectable human apoA-I and very low levels of HDL cholesterol (**Table 4**, **Fig. 4**). WT apoA-I-expressing mice had a plasma apoA-I level of 154 mg/dl and a HDL cholesterol level of 80 mg/dl, while apoA-I_M-expressing mice had slightly lower plasma apoA-I values, with 43% ± 9% (n = 3) of the apoA-I_M being in the dimeric state (**Fig. 5**). ApoA-I_M-expressing mice also had substantially reduced levels of plasma lipids compared with WT apoA-I-expressing mice, with the exception of triglycerides, which were increased (Table 4). The increase in plasma triglycerides in the mice was comparable to the increase in triglycerides seen in the human apoA-I_M carriers (52), but the cause of this is undetermined at this time. R173S apoA-I-expressing mice also had reduced HDL and total cholesterol levels compared with WT apoA-I-expressing mice, but higher levels than apoA-I_M-expressing mice. R173S apoA-I-expressing mice had a triglyceride level and a percentage of cholesteryl ester in plasma similar to WT apoA-I-expressing mice. R173K apoA-I-expressing mice had similar lipid and apoA-I levels to mice expressing WT apoA-I. At 6 weeks, upon necropsy, hepatic apoA-I mRNA abundance in the WT, apoA-I_M, R173S, and R173K apoA-I groups was not significantly different (data not shown). Plasma samples analyzed by FPLC (data not shown) gave HDL peaks that eluted at the same point with intensities proportional to the levels of HDL cholesterol (Table 4).

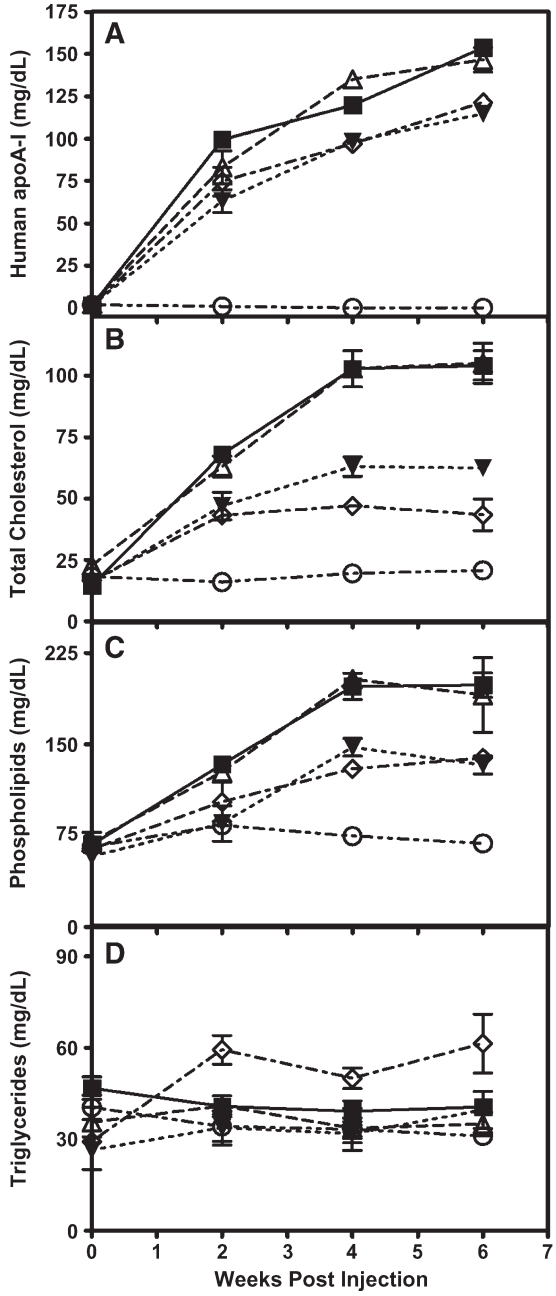

Fig. 4. Plasma apoA-I and lipid levels in mice expressing the human apoA-I variants. ApoA-I-null mice were infected with 1.0×10^{12} viral particles of AAV expressing: WT apoA-I (squares), apoA-I_{Milano} (diamonds), R173S apoA-I (closed triangles), R173K apoA-I (open triangles), and LacZ as a control (circles). Mice were periodically bled after a 4-h fast and the plasma assayed for human apoA-I levels (A), cholesterol levels (B), phospholipids (C), and triglycerides (D).

HDL particle size and composition

Western blot analysis of plasma using nondenaturing gradient gels revealed that mice expressing WT apoA-I, R173S apoA-I, and R173K apoA-I all produced a single HDL_2-sized particle that was approximately 12 nm in diameter (**Fig. 6**). In contrast, apoA-I_M-expressing mice produced equal amounts of two separate HDL particles, an HDL_2-sized particle 12 nm in diameter, and a smaller HDL_3-sized particle 10 nm in diameter. HDL compositions were obtained by treating plasma samples with polyethylene glycol to precipitate any apoB-containing lipoproteins. Subsequent analysis of the samples indicated that the HDL lipid compositions of all the variants were remarkably similar on a molar basis (**Table 5**) despite the difference in size of the apoA-I_M HDL particle. Analysis of the protein composition of isolated HDL from WT apoA-I-expressing mice indicated that apoA-I was the only protein with no apoA-II or apoE detected (**Fig. 7**). For HDL isolated from apoA-I_M-expressing mice, apoA-I accounted for approximately 95% of the total protein and a

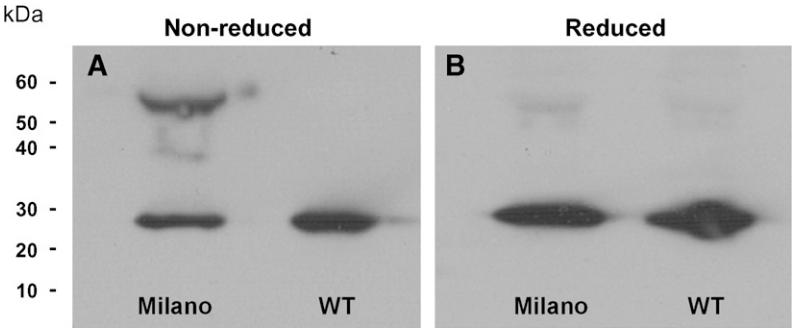

Fig. 5. Western blot analysis of WT and apoA-I_M in mouse plasma. Seven weeks after AAV injection, apoA-I-null mice were bled and 1 μl of plasma was run on a 4–12% SDS-PAGE Tris-glycine gel. The samples were transferred to nitrocellulose and Western blotted for human apoA-I. Monomeric apoA-I_M had an apparent molecular mass of approximately 28 kDa, while dimeric apoA-I_M had a molecular mass of approximately 56 kDa. Nonreduced (A) and reduced (B) conditions.

small amount of apoE was present (as analyzed by scanning densitometry using Image J version 1.31).

DISCUSSION

Heterozygous carries of the apoA-I_M mutation have reduced plasma levels of apoA-I and HDL cholesterol but do not display the increase in cardiovascular disease that would be expected for such levels (10). This observation has led to intense interest in the apoA-I_M mutation as a potential therapeutic agent to treat cardiovascular disease (25, 26). However, a fundamental understanding of why apoA-I_M behaves as it does is lacking. To determine if the removal of the arginine at position 173 (and loss of positive charge) or the introduction of a cysteine residue (with the potential for disulfide bond formation) was responsible for the altered functional aspects of apoA-I_M, we generated two engineered variants of apoA-I_M with different residues at position 173. The first, R173S apoA-I, is a mutant structurally similar to apoA-I_M but, unlike the sulfhydryl group of the cysteine residue in apoA-I_M that has the ability to form disulfide bonds with other cysteine residues, the hydroxyl group of the serine in R173S apoA-I is unable to do so. The second mutation, R173K apoA-I, is a conservative mutation that maintains the positive charge at position 173 of WT apoA-I.

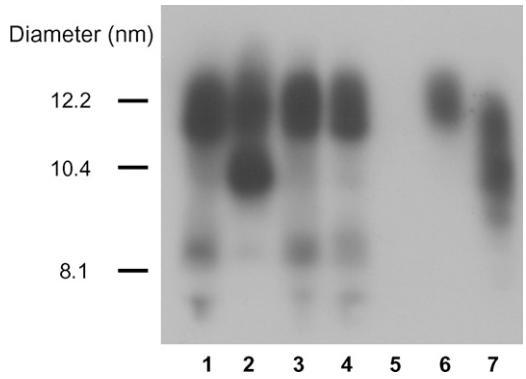

Fig. 6. Particle size analysis of HDL from mice expressing the human apoA-I variants. Three weeks after AAV injection, apoA-I-null mice were bled and 1 μl of plasma was run on a 4–20% Tris-glycine nondenaturing gradient gel. The samples were transferred to nitrocellulose and Western blotted for human apoA-I. Lane 1, WT apoA-I; lane 2, apoA-I_{Milano}; lane 3, R173S apoA-I; lane 4, R173K apoA-I; lane 5, LacZ; lane 6, human HDL_2; lane 7, human HDL_3.

Effects of mutations at position 173 on apoA-I structure and lipid binding properties

Analysis of the X-ray crystal structure of lipid-free apoA-I (8) using the Protein Explorer 2.8 software (University of Massachusetts, www.proteinexplorer.org) indicates that arginine 173 forms an intrahelical salt bridge with glutamic acid 169 in the N-terminal helical bundle domain of the protein. Assuming that the α-helix spanning residue 173 is also present in a lipid-free apoA-I molecule in dilute solution, it follows that this ion pair between the two residues separated by a single turn of helix is likely to be maintained. Thus, the substitution of an uncharged serine residue for the positively charged arginine residue in the R173S apoA-I mutation would be expected to disrupt the salt bridge that is present in the WT protein and thereby destabilize the protein. On the other hand, maintenance of the positive charge by introduction of a lysine residue would be expected to have no effect on the interaction. Elimination of the positive charge by the R173S mutation alters the structure and stability of the protein, as indicated by reductions in the midpoints of thermal, GdnHCl, and urea denaturation (Table 2, Figs. 1 and 2) and increases in exposed hydrophobic regions measured by ANS fluorescence (Table 1, Fig. 3). Substituting a cysteine for the arginine in the apoA-I_M mutation further destabilizes the protein. At physiological pH, the cysteine residue is slightly negatively charged (pK_a = 8.3), unlike the arginine residue, which is positively charged (pK_a = 12.5), or the serine residue, which has no charge (i.e., it is nonionizable). It can be inferred that the slightly negatively charged sulfhydryl group in the cysteine residue actively repels the negatively charged glutamic acid residue 169 that would form a salt bridge with the arginine at position 173 in the WT protein. This inference is validated by the fact that thermal denaturation and urea denaturation, both of which take into account electrostatic interactions, show that monomeric apoA-I_M is less stable than dimeric apoA-I_M (Table 2), indicating the presence of a destabilizing electrostatic interaction in monomeric apoA-I_M that is removed when the covalent disulfide bond is formed in dimeric apoA-I_M at position 173. However, when monomeric and dimeric apoA-I_M are denatured by GdnHCl, which only measures the stability conferred by hydrophobic and nonionic interactions, monomeric apoA-I_M is more stable than dimeric apoA-I_M.

TABLE 5. Lipid compositions of HDL in mice expressing human ApoA-I variants

HDL[a]	Phospholipid:apoA-I (mol:mol)	Free Cholesterol:apoA-I (mol:mol)	Cholesteryl Ester:apoA-I (mol:mol)	Triglyceride:apoA-I (mol:mol)
WT	70 ± 24	9 ± 1	26 ± 9	1 ± 1
Milano	66 ± 14	11 ± 1	30 ± 10	2 ± 2
R173S	59 ± 13	6 ± 2	21 ± 4	1 ± 1
R173K	64 ± 11	7 ± 1	27 ± 9	1 ± 1

[a] Respective AAV injected into apoA-I$^{-/-}$ mice with a dose of 1.0×10^{12} viral particles. All data taken from week 6 postinfection and represent a mean ± SD (n = 3–7).

The presence of the cysteine residue at position 173 significantly alters the structure and decreases the stability of the monomeric R173C variant compared with the R173S variant, as reflected by the changes in the denaturation parameters listed in Table 2. Further support for the involvement of position 173 in a stabilizing salt bridge in WT apoA-I comes from the observation that reversal of the charge by the mutation R173E reduces the midpoint of thermal denaturation to 51°C (data not shown), which is lower than the value for monomeric apoA-I_M (Table 2). The above considerations of the electrostatic interactions of R173 are likely to also apply to apoA-I in the lipid-bound state. Thus, analysis using Protein Explorer 2.8 of the crystal structure of a truncated form of apoA-I, apoA-I Δ1-43, which adopts a lipid bound-like conformation (53), indicates that the intrahelix R173-E169 interaction also occurs in this state.

When apoA-I binds to lipid or lipoprotein particles, the C-terminal domain binds first accompanied by an increase in α-helix content in this region (54). Subsequently, α-helices in the N-terminal region of the apoA-I molecule interact with lipid (55, 56). In light of the two-domain tertiary structure of apoA-I (7, 8, 57), we have proposed a two-step mechanism for apoA-I binding to a lipid surface; the initial C-terminal domain binding is followed by opening of the helix bundle of the N-terminal domain and interaction of these α-helices with lipid (7, 54, 58). The apoA-I_M mutation, and the engineered R173 variants, are located in the N-terminal domain of apoA-I and, as such, affect the ability of apoA-I to interact with lipid particles by influencing the stability of the α-helix bundle. Consistent with this concept, the decreased stability of the N-terminal helix bundle domain in the R173S and R173C apoA-I variants (Table 2) leads to enhanced rates of interaction of α-helices in this domain with the phospholipid particle surface (see the enhanced enthalpy decay rates listed in Table 3). Furthermore, the binding enthalpies listed in Table 3 indicate that the affinity of apoA-I for the surface of a stable egg PC SUV is reduced by nonconservative amino acid substitutions at position 173. Thus, the R173S and R173C variants are expected to bind less well to the phospholipid surface of HDL particles so that their presence in the lipid-free/poor pool of apoA-I is increased.

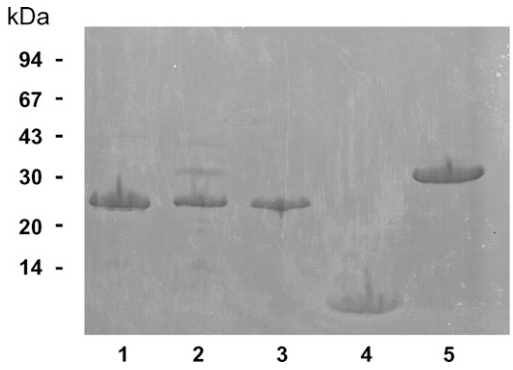

Fig. 7. Protein composition analysis of isolated WT and apoA-I_M HDL. HDL was isolated from the plasma of mice expressing WT apoA-I and apoA-I_M by ultracentrifugation and analyzed on a reducing 8–25% SDS-PAGE gel. Lane 1, WT apoA-I HDL; lane 2, apoA-I_M HDL; lane 3, human apoA-I; lane 4, human apoA-II; lane 5, mouse apoE.

The lipid binding properties of apoA-I are also important for the formation of nascent HDL particles via the ABCA1 reaction. In this process, the solubilization of exovesiculated domains of cell plasma membrane is rate-limiting for the formation of discoidal HDL particles (59). Consequently, the effects of variations in the apoA-I molecule on the ability to solubilize phospholipid bilayers (as in DMPC multilamellar vesicles) are correlated with the ability to efflux cellular lipids via the ABCA1 pathway and create nascent HDL particles. Since the substitution of arginine at position 173 in the apoA-I molecule with lysine, serine, or cysteine has no effect on the ability of the proteins in the monomeric state to solubilize DMPC multilamellar vesicles (Table 3), it follows that these variants should all participate equally well in the ABCA1 reaction to form nascent HDL particles. Indeed, earlier work demonstrated that monomeric apoA-I_M is as effective as WT apoA-I at forming HDL particles via the ABCA1 reaction (60). It is not known how dimeric apoA-I_M participates in the ABCA1 reaction, but the fact that the dimeric form of apoA-I_M had a 2-fold slower rate of clearance compared with WT apoA-I is probably due to steric hindrances imposed by the disulfide bond. In the DMPC clearance assay, apoA-I binds to the lipid surface, undergoes a conformational change, and then solubilizes a portion of the lipid (36). It follows that the rate of formation of nascent HDL particles containing dimeric apoA-I_M via the ABCA1 reaction may be relatively slow in vivo, contributing to the reduction in plasma apoA-I_M levels (Table 4). This effect occurs either because of steric hindrance to helix bundle opening associated with the presence of the disulfide bond or perhaps because of interference between the two molecules in the apoA-I_M dimer as they bind to the lipid surface. In vivo, approximately 40% of apoA-I_M generated via AAV-mediated gene transfer

is in the dimeric state (Fig. 5) and presumably would have lipid interactions altered in this fashion.

Effects of mutations of R173 in apoA-I on HDL composition

AAVs were generated for each apoA-I variant and subsequently used to infect apoA-I-null mice. ApoA-I-null mice were used to maintain the simplicity of the system and allow the study of the apoA-I_M mutation without the confounding factors of the presence of murine apoA-I, WT human apoA-I, or other potential heterodimer partners of apoA-I_M, such as human apoA-II and apoE3; murine apoA-II and apoE do not contain cysteine residues and thus cannot form covalently bonded heterodimers with apoA-I_M. Thus, this in vivo system was not intended to recreate the situation in human apoA-I_M probands but rather give a model system to elucidate apoA-I structure-function relationships. Plasma apoA-I levels for WT apoA-I and the R173K variant were similar, but mice with the R173S and R173C variants had lower levels of apoA-I compared with WT apoA-I (Fig. 4, Table 4). Real-time PCR has shown that AAV induces equal amounts of the WT apoA-I and apoA-I variant mRNA in mouse livers (data not shown), indicating that production of WT apoA-I and the apoA-I variants is similar. As previously discussed, the formation of nascent HDL particles via the ABCA1 reaction is expected to be normal for all of the monomeric apoA-I variants studied, leading to the conclusion that the lower plasma apoA-I level of the R173S variant may be due to enhanced turnover of plasma apoA-I by clearance in the kidney (61–63). The reduced lipid affinity of the R173S and R173C apoA-I variants results in a larger pool of lipid-free apoA-I that is susceptible to rapid catabolism, as has been previously shown for apoA-I_M (64). As discussed above, the ABCA1 reaction for dimeric apoA-I_M may also be slower, contributing to the lower plasma apoA-I_M levels.

The HDL lipid particle compositions for all of the apoA-I variants were very similar (Table 5) as were the protein compositions (Fig. 7). However, apoA-I_M HDL had a bimodal size distribution with equal amounts of HDL_2 and HDL_3, whereas all other apoA-I variants formed primarily HDL_2 (Fig. 6). The smaller apoA-I_M HDL particle size is likely due to the presence of apoA-I_M homodimer, which accounts for approximately 40% of apoA-I_M mass in mice expressing apoA-I_M via AAV-mediated gene transfer (Fig. 5) and not due to other apoproteins being present (Fig. 7). WT apoA-I can form HDL with two, three, four, or more apoA-I molecules per particle, while dimeric apoA-I_M can only generate HDL particles with even numbers of apoA-I molecules (two, four, six, etc.), which is expected to constrain the HDL particle size possibilities. Consistent with this, previous work showed that apoA-I_M restricts HDL particle size in vivo (64) and that this restriction is due to the formation of dimeric apoA-I_M (65).

Whether or not alterations in HDL caused by the R173C mutation alter the anti-atherogenic properties of HDL compared with WT apoA-I is still controversial. Several recent mouse studies have reached conflicting results. An apoA-I_M knockin mouse strain was crossed with an atherosclerosis-susceptible human apoB/apoA-II mouse model, and apoA-I_M was found to have no protective advantage over WT apoA-I (23). However, a study in which bone marrow transplantation in apoA-I and apoE double-knockout mice using bone marrow that had been transduced with a retroviral vector expressing WT apoA-I or apoA-I_M demonstrated that apoA-I_M reduced atherosclerosis to a greater extent than WT apoA-I (19). However, when LDL receptor-deficient mice were infected with AAV expressing either WT apoA-I or apoA-I_M and fed a Western diet for 8 weeks, there was no difference in lesion development (24).

In summary, the removal of the arginine residue and the introduction of the cysteine residue in the apoA-I_M mutation contribute to the altered physical properties and in vivo metabolism of the protein. Both alterations involved in the apoA-I_M mutation help to destabilize the protein and modify the interactions with lipids, resulting in lower plasma HDL cholesterol and apoA-I values in vivo, as well as an altered HDL particle size distribution.

REFERENCES

1. Davidson, W. S., and T. B. Thompson. 2007. The structure of apolipoprotein A-I in high density lipoproteins. *J. Biol. Chem.* **282:** 22249–22253.
2. Lewis, G. F., and D. J. Rader. 2005. New insights into the regulation of HDL metabolism and reverse cholesterol transport. *Circ. Res.* **96:** 1221–1232.
3. Yancey, P. G., A. E. Bortnick, G. Kellner-Weibel, M. De La Llera-Moya, M. C. Phillips, and G. H. Rothblat. 2003. Importance of different pathways of cellular cholesterol efflux. *Arterioscler. Thromb. Vasc. Biol.* **23:** 712–719.
4. Curtiss, L. K., D. T. Valenta, N. J. Hime, and K. A. Rye. 2006. What is so special about apolipoprotein AI in reverse cholesterol transport? *Arterioscler. Thromb. Vasc. Biol.* **26:** 12–19.
5. Weisgraber, K. H., S. C. Rall, T. P. Bersot, R. W. Mahley, G. Franceschini, and C. R. Sirtori. 1983. Apolipoprotein A-I milano - detection of normal A-I in affected subjects and evidence for a cysteine for arginine substitution in the variant A-I. *J. Biol. Chem.* **258:** 2508–2513.
6. Rocco, A. G., L. Mollica, E. Gianazza, L. Calabresi, G. Franceschini, C. R. Sirtori, and I. Eberini. 2006. A model structure for the heterodimer apoA-I-Milano-apoA-II supports its peculiar susceptibility to proteolysis. *Biophys. J.* **91:** 3043–3049.
7. Saito, H., P. Dhanasekaran, D. Nguyen, P. Holvoet, S. Lund-Katz, and M. C. Phillips. 2003. Domain structure and lipid interaction in human apolipoproteins A-I and E, a general model. *J. Biol. Chem.* **278:** 23227–23232.
8. Ajees, A. A., G. M. Anantharamaiah, V. K. Mishra, M. M. Hussain, and H. M. K. Murthy. 2006. Crystal structure of human apolipoprotein A-I: insights into its protective effect against cardiovascular diseases. *Proc. Natl. Acad. Sci. USA.* **103:** 2126–2131.
9. Sorci-Thomas, M. G., and M. J. Thomas. 2002. The effects of altered apolipoprotein A-I structure on plasma HDL concentration. *Trends Cardiovasc. Med.* **12:** 121–128.
10. Sirtori, C. R., L. Calabresi, G. Franceschini, D. Baldassarre, M. Amato, J. Johansson, M. Salvetti, C. Monteduro, R. Zulli, M. L. Muiesan, et al. 2001. Cardiovascular status of carriers of the apolipoprotein A-I_{Milano} mutant - the Limone sul Garda study. *Circulation.* **103:** 1949–1954.
11. Calabresi, L., G. Franceschini, A. Burkybile, and A. Jonas. 1997. Activation of lecithin cholesterol acyltransferase by a disulfide-linked apolipoprotein A-I dimer. *Biochem. Biophys. Res. Commun.* **232:** 345–349.
12. Roma, P., R. E. Gregg, M. S. Meng, R. Ronan, L. A. Zech, G. Franceschini, C. R. Sirtori, and H. B. Brewer, Jr. 1993. In vivo metabolism of a mutant form of apolipoprotein A-I, apo A-I_{Milano}, associated with familial hypoalphalipoproteinemia. *J. Clin. Invest.* **91:** 1445–1452.
13. Perez-Mendez, O., E. Bruckert, G. Franceschini, N. Duhal, B. Lacroix, J. P. Bonte, C. Sirtori, J. C. Fruchart, G. Turpin, and G. Luc. 2000. Metabolism of apolipoproteins AI and AII in subjects carrying

similar apoAI mutations, apoAI Milano and apoAI Paris. *Atherosclerosis.* **148:** 317–326.
14. Gualandri, V., G. Franceschini, C. R. Sirtori, G. Gianfranceschi, G. B. Orsini, A. Cerrone, and A. Menotti. 1985. AIMilano apoprotein identification of the complete kindred and evidence of a dominant genetic transmission. *Am. J. Hum. Genet.* **37:** 1083–1097.
15. Gomaraschi, M., D. Baldassarre, M. Amato, S. Eligini, P. Conca, C. R. Sirtori, G. Franceschini, and L. Calabresi. 2007. Normal vascular function despite low levels of high-density lipoprotein cholesterol in carriers of the apolipoprotein A-I-Milano mutant. *Circulation.* **116:** 2165–2172.
16. Franceschini, G., L. Calabresi, G. Chiesa, C. Parolini, C. R. Sirtori, M. Canavesi, and F. Bernini. 1999. Increased cholesterol efflux potential of sera from ApoA-I_{Milano} carriers and transgenic mice. *Arterioscler. Thromb. Vasc. Biol.* **19:** 1257–1262.
17. Calabresi, L., M. Canavesi, F. Bernini, and G. Franceschini. 1999. Cell cholesterol efflux to reconstituted high-density lipoproteins containing the apolipoprotein A-I_{Milano} dimer. *Biochemistry.* **38:** 16307–16314.
18. Bielicki, J. K., and M. N. Oda. 2002. Apolipoprotein A-I_{Milano} and apolipoprotein A-I_{Paris} exhibit an antioxidant activity distinct from that of wild-type apolipoprotein A-I. *Biochemistry.* **41:** 2089–2096.
19. Wang, L., B. G. Sharifi, T. Pan, L. Song, A. Yukht, and P. K. Shah. 2006. Bone marrow transplantation shows superior atheroprotective effects of gene therapy with apolipoprotein A-I Milano compared with wild-type apolipoprotein A-I in hyperlipidemic mice. *J. Am. Coll. Cardiol.* **48:** 1459–1468.
20. Parolini, C., M. Marchesi, P. Lorenzon, M. Castano, E. Balconi, L. Miragoli, L. Chaabane, A. Morisetti, V. Lorusso, B. J. Martin, et al. 2008. Dose-related effects of repeated ETC-216 (recombinant apolipoprotein A-I-Milano/1-palmitoyl-2-oleoyl phosphatidylcholine complexes) administrations on rabbit lipid-rich soft plaques - In vivo assessment by intravascular ultrasound and magnetic resonance imaging. *J. Am. Coll. Cardiol.* **51:** 1098–1103.
21. Ibanez, B., G. Vilahur, G. Cimmino, W. S. Speidl, A. Pinero, B. G. Choi, M. U. Zafar, C. G. Santos-Gallego, B. Krause, L. Badirnon, et al. 2008. Rapid change in plaque size, composition, and molecular footprint after recombinant apolipoprotein A-I-Milano (ETC-216) administration - magnetic resonance imaging study in an experimental model of atherosclerosis. *J. Am. Coll. Cardiol.* **51:** 1104–1109.
22. Marchesi, M., E. A. Booth, G. Rossoni, R. A. Garcia, K. R. Hill, C. R. Sirtori, C. L. Bisgaier, and B. R. Lucchesi. 2008. Apolipoprotein A-I-Milano/POPC complex attenuates post-ischemic ventricular dysfunction in the isolated rabbit heart. *Atherosclerosis.* **197:** 572–578.
23. Parolini, C., G. Chiesa, E. Gong, S. Caligari, M. M. Cortese, T. Koga, T. M. Forte, and E. M. Rubin. 2005. Apolipoprotein A-I and the molecular variant apoA-IMilano: evaluation of the antiatherogenic effects in knock-in mouse model. *Atherosclerosis.* **183:** 222–229.
24. Lebherz, C., J. Sanmiguel, J. Wilson, and D. Rader. 2007. Gene transfer of wild-type apoA-I and apoA-I Milano reduce atherosclerosis to a similar extent. *Cardiovasc. Diabetol.* **6:** 15.
25. Nissen, S. E., T. Tsunoda, E. M. Tuzcu, P. Schoenhagen, C. J. Cooper, M. Yasin, G. M. Eaton, M. A. Lauer, W. S. Sheldon, C. L. Grines, et al. 2003. Effect of recombinant apoA-I milano on coronary atherosclerosis in patients with acute coronary syndromes: a randomized controlled trial. *JAMA.* **290:** 2292–2300.
26. Nicholls, S. J., E. M. Tuzcu, T. Crowe, I. Sipahi, P. Schoenhagen, S. Kapadia, S. L. Hazen, C. C. Wun, M. Norton, F. Ntanios, et al. 2006. Relationship between cardiovascular risk factors and atherosclerotic disease burden measured by intravascular ultrasound. *J. Am. Coll. Cardiol.* **47:** 1967–1975.
27. Kitajima, K., D. H. L. Marchadier, H. Burstein, and D. J. Rader. 2006. Persistent liver expression of murine apoA-1 using vectors based on adeno-associated viral vectors serotypes 5 and 1. *Atherosclerosis.* **186:** 65–73.
28. Morrow, J. A., K. S. Arnold, and K. H. Weisgraber. 1999. Functional characterization of apolipoprotein E isoforms overexpressed in *Escherichia coli*. *Protein Expr. Purif.* **16:** 224–230.
29. Saito, H., P. Dhanasekaran, D. Nguyen, E. Deridder, P. Holvoet, S. Lund-Katz, and M. C. Phillips. 2004. Alpha-helix formation Is required for high affinity binding of human apolipoprotein A-I to lipids. *J. Biol. Chem.* **279:** 20974–20981.
30. Morrisett, J. D., J. S. David, H. J. Pownall, and A. M. Gotto, Jr. 1973. Interaction of an apolipoprotein (Apolp-Alanine) with phosphatidylcholine. *Biochemistry.* **12:** 1290–1299.
31. Tanaka, M., P. Dhanasekaran, D. Nguyen, S. Ohta, S. Lund-Katz, M. C. Phillips, and H. Saito. 2006. Contributions of the N- and C-terminal helical segments to the lipid-free structure and lipid interaction of apolipoprotein A-I. *Biochemistry.* **45:** 10351–10358.
32. Acharya, P., M. L. Segall, M. Zaiou, J. Morrow, K. H. Weisgraber, M. C. Phillips, S. Lund-Katz, and J. Snow. 2002. Comparison of the stabilities and unfolding pathways of human apolipoprotein E isoforms by differential scanning calorimetry and circular dichroism. *Biochim. Biophys. Acta.* **1584:** 9–19.
33. Tanaka, M., C. Vedhachalam, T. Sakamoto, P. Dhanasekaran, M. C. Phillips, S. Lund-Katz, and H. Saito. 2006. Effect of carboxyl-terminal truncation on structure and lipid interaction of human apolipoprotein E4. *Biochemistry.* **45:** 4240–4247.
34. Eftink, M. R. 2000. Use of fluorescence spectroscopy as thermodynamics tool. *Methods Enzymol.* **323:** 459–473.
35. Sparks, D. L., S. Lund-Katz, and M. C. Phillips. 1992. The charge and structural stability of apolipoprotein A-I in discoidal and spherical recombinant high density lipoprotein particles. *J. Biol. Chem.* **267:** 25839–25847.
36. Segall, M. L., P. Dhanasekaran, F. Baldwin, G. M. Anantharamaiah, K. H. Weisgraber, M. C. Phillips, and S. Lund-Katz. 2002. Influence of apoE domain structure and polymorphism on the kinetics of phospholipid vesicle solubilization. *J. Lipid Res.* **43:** 1688–1700.
37. Kitajima, K., D. H. L. Marchadier, G. C. Miller, G. P. Gao, J. M. Wilson, and D. J. Rader. 2006. Complete prevention of atherosclerosis in ApoE-deficient mice by hepatic human ApoE gene transfer with adeno-associated virus serotypes 7 and 8. *Arterioscler. Thromb. Vasc. Biol.* **26:** 1852–1857.
38. Sandalon, Z., E. M. Bruckheimer, K. H. Lustig, L. C. Rogers, R. W. Peluso, and H. Burstein. 2004. Secretion of a TNFR: Fc fusion protein following pulmonary administration of pseudotyped adeno-associated virus vectors. *J. Virol.* **78:** 12355–12365.
39. Gao, G., L. H. Vandenberghe, and J. M. Wilson. 2005. New recombinant serotypes of AAV vectors. *Curr. Gene Ther.* **5:** 285–297.
40. Asztalos, B. F., M. de la Llera-Moya, G. E. Dallal, K. V. Horvath, E. J. Schaefer, and G. H. Rothblat. 2005. Differential effects of HDL subpopulations on cellular ABCA1- and SR-BI-mediated cholesterol efflux. *J. Lipid Res.* **46:** 2246–2253.
41. Lund-Katz, S., and M. C. Phillips. 1986. Packing of cholesterol molecules in human low-density-lipoprotein. *Biochemistry.* **25:** 1562–1568.
42. Franceschini, G., G. Vecchio, G. Gianfranceschi, D. Magani, and C. R. Sirtori. 1985. Apolipoprotein AI Milano. Accelerated binding and dissociation from lipids of a human apolipoprotein variant. *J. Biol. Chem.* **260:** 16321–16325.
43. Zhu, X., G. Wu, W. Zeng, H. Xue, and B. Chen. 2005. Cysteine mutants of human apolipoprotein A-I: a study of secondary structural and functional properties. *J. Lipid Res.* **46:** 1303–1311.
44. Calabresi, L., G. Vecchio, R. Longhi, E. Gianazza, G. Palm, H. Wadensten, A. Hammarström, A. Olsson, A. Karlström, T. Sejlitz, et al. 1994. Molecular characterization of native and recombinant apolipoprotein A-I_{Milano} dimer. The introduction of an interchain disulfide bridge remarkably alters the physicochemical properties of apolipoprotein A-I. *J. Biol. Chem.* **269:** 32168–32174.
45. Monera, O. D., C. M. Kay, and R. S. Hodges. 1994. Protein denaturation with guanidine-hydrochloride or urea provides a different estimate of stability depending on the contributions of electrostatic interactions. *Protein Sci.* **3:** 1984–1991.
46. Beckstead, J. A., B. L. Block, J. K. Bielicki, C. M. Kay, M. N. Oda, and R. O. Ryan. 2005. Combined N- and C-terminal truncation of human apolipoprotein A-I yields a folded, functional central domain. *Biochemistry.* **44:** 4591–4599.
47. Rogers, D. P., C. G. Brouillette, J. A. Engler, S. W. Tendian, L. Roberts, V. K. Mishra, G. M. Anantharamaiah, S. Lund-Katz, M. C. Phillips, and M. J. Ray. 1997. Truncation of the amino terminus of human apolipoprotein A-I substantially alters only the lipid-free conformation. *Biochemistry.* **36:** 288–300.
48. Calabresi, L., G. Vecchio, F. Frigerio, L. Vavassori, C. R. Sirtori, and G. Franceschini. 1997. Reconstituted high-density lipoproteins with a disulfide-linked apolipoprotein A-I dimer: evidence for restricted particle size heterogeneity. *Biochemistry.* **36:** 12428–12433.
49. Saito, H., P. Dhanasekaran, F. Baldwin, K. H. Weisgraber, S. Lund-Katz, and M. C. Phillips. 2001. Lipid binding-induced conformational change in human apolipoprotein E - evidence for two lipid-bound states on spherical particles. *J. Biol. Chem.* **276:** 40949–40954.
50. Derksen, A., D. Gantz, and D. M. Small. 1996. Calorimetry of apolipoprotein-A1 binding to phosphatidylcholine-triolein-cholesterol emulsions. *Biophys. J.* **70:** 330–338.

51. Arnulphi, C., L. H. Jin, M. A. Tricerri, and A. Jonas. 2004. Enthalpy-driven apolipoprotein A-I and lipid bilayer interaction indicating protein penetration upon lipid binding. *Biochemistry.* **43:** 12258–12264.
52. Franceschini, G., C. R. Sirtori, E. Bosisio, V. Gualandri, G. B. Orsini, A. M. Mogavero, and A. Capurso. 1985. Relationship of the phenotypic-expression of the A-Imilano apoprotein with plasma-lipid and lipoprotein patterns. *Atherosclerosis.* **58:** 159–174.
53. Borhani, D. W., D. P. Rogers, J. A. Engler, and C. G. Brouillette. 1997. Crystal structure of truncated human apolipoprotein A-I suggests a lipid-bound conformation. *Proc. Natl. Acad. Sci. USA.* **94:** 12291–12296.
54. Oda, M. N., T. M. Forte, R. O. Ryan, and J. C. Voss. 2003. The C-terminal domain of apolipoprotein A-I contains a lipid-sensitive conformational trigger. *Nat. Struct. Biol.* **10:** 455–460.
55. Rogers, D. P., L. M. Roberts, J. Lebowitz, G. Datta, G. M. Anantharamaiah, J. A. Engler, and C. G. Brouillette. 1998. The lipid-free structure of apolipoprotein A-I: effects of amino-terminal deletions. *Biochemistry.* **37:** 11714–11725.
56. Rogers, D. P., L. M. Roberts, J. Lebowitz, J. A. Engler, and C. G. Brouillette. 1998. Structural analysis of apolipoprotein A-I: effects of amino- and carboxy-terminal deletions on the lipid-free structure. *Biochemistry.* **37:** 945–955.
57. Saito, H., S. Lund-Katz, and M. C. Phillips. 2004. Contributions of domain structure and lipid interaction to the functionality of exchangeable human apolipoproteins. *Prog. Lipid Res.* **43:** 350–380.
58. Kono, M., Y. Okumura, M. Tanaka, D. Nguyen, P. Dhanasekaran, S. Lund-Katz, M. C. Phillips, and H. Saito. 2008. Conformational flexibility of the N-terminal domain of apolipoprotein A-I bound to spherical lipid particles. *Biochemistry.* **47:** 11340–11347.
59. Vedhachalam, C., P. T. Duong, M. Nickel, D. Nguyen, P. Dhanasekaran, H. Saito, G. H. Rothblat, S. Lund-Katz, and M. C. Phillips. 2007. Mechanism of ATP-binding cassette transporter A1-mediated cellular lipid efflux to apolipoprotein A-I and formation of high density lipoprotein particles. *J. Biol. Chem.* **282:** 25123–25130.
60. Weibel, G. L., E. T. Alexander, M. R. Joshi, D. J. Rader, S. Lund-Katz, M. C. Phillips, and G. H. Rothblat. 2007. Wild-type ApoA-I and the Milano variant have similar abilities to stimulate cellular lipid mobilization and efflux. *Arterioscler. Thromb. Vasc. Biol.* **27:** 2022–2029.
61. Timmins, J. M., J. Y. Lee, E. Boudyguina, K. D. Kluckman, L. R. Brunham, A. Mulya, A. K. Gebre, J. M. Coutinho, P. L. Colvin, T. L. Smith, et al. 2005. Targeted inactivation of hepatic Abca1 causes profound hypoalphalipoproteinemia and kidney hypercatabolism of apoA-I. *J. Clin. Invest.* **115:** 1333–1342.
62. Moestrup, S. K., and L. B. Nielsen. 2005. The role of the kidney in lipid metabolism. *Curr. Opin. Lipidol.* **16:** 301–306.
63. Lee, J. Y., J. M. Timmins, A. Mulya, T. L. Smith, Y. W. Zhu, E. M. Rubin, J. W. Chisholm, P. L. Colvin, and J. S. Parks. 2005. HDLs in apoA-I transgenic Abca1 knockout mice are remodeled normally in plasma but are hypercatabolized by the kidney. *J. Lipid Res.* **46:** 2233–2245.
64. Bielicki, J. K., T. M. Forte, M. R. McCall, L. J. Stoltzfus, G. Chiesa, C. R. Sirtori, G. Franceschini, and E. M. Rubin. 1997. High density lipoprotein particle size restriction in apolipoprotein A-I_{Milano} transgenic mice. *J. Lipid Res.* **38:** 2314–2321.
65. Favari, E., M. Gomaraschi, I. Zanotti, F. Bernini, M. Lee-Rueckert, P. T. Kovanen, C. R. Sirtori, G. Franceschini, and L. Calabresi. 2007. A unique protease-sensitive high density lipoprotein particle containing the apolipoprotein A-I-Milano dimer effectively promotes ATP-binding cassette A1-mediated cell cholesterol efflux. *J. Biol. Chem.* **282:** 5125–5132.